

PAPER

## Synergistic effect of W incorporation and pulsed current mode on wear and tribocorrosion resistance of coatings grown by plasma electrolytic oxidation on 7075 Al alloy

To cite this article: Amirhossein Toulabifard *et al* 2019 *Mater. Res. Express* **6** 106502

View the [article online](#) for updates and enhancements.



**IOP | ebooks™**

Bringing you innovative digital publishing with leading voices to create your essential collection of books in STEM research.



Start exploring the collection - download the first chapter of every title for free.

# Materials Research Express



## PAPER

# Synergistic effect of W incorporation and pulsed current mode on wear and tribocorrosion resistance of coatings grown by plasma electrolytic oxidation on 7075 Al alloy

Amirhossein Toulabifard<sup>1</sup> , Amin Hakimizad<sup>1</sup>, Francesco Di Franco<sup>2</sup>, Keyvan Raeissi<sup>1,3</sup>  and Monica Santamaria<sup>2,3</sup>

<sup>1</sup> Department of Materials Engineering, Isfahan University of Technology, Isfahan 84156-83111, Iran

<sup>2</sup> Electrochemical Materials Science Laboratory, Dipartimento di Ingegneria, Università di Palermo, Viale delle Scienze, Ed. 6, 90128, Palermo, Italy

<sup>3</sup> Authors to whom any correspondence should be addressed.

E-mail: [k\\_raeissi@cc.iut.ac.ir](mailto:k_raeissi@cc.iut.ac.ir), [k\\_raeissi@yahoo.com](mailto:k_raeissi@yahoo.com) and [monica.santamaria@unipa.it](mailto:monica.santamaria@unipa.it)

**Keywords:** 7075 Al alloy, duty cycles, tungstate, bipolar waveforms, wear, tribocorrosion

RECEIVED  
4 May 2019

REVISED  
10 July 2019

ACCEPTED FOR PUBLICATION  
26 July 2019

PUBLISHED  
7 August 2019

## Abstract

Ceramic coatings were grown by plasma electrolytic oxidation on 7075 Al alloy using unipolar and bipolar pulsed current waveforms with 20 and 40% cathodic duty cycles, from a silicate-based bath without and with the addition of Na<sub>2</sub>WO<sub>4</sub>. Pancake-like morphology was dominant on the coatings grown by unipolar waveform, while the bipolar waveforms promoted volcano-like morphology, increased the roughness of the coating surface and the formation of more compact layers. The coatings produced using the bipolar waveforms provided higher resistances toward both tribocorrosion and dry sliding conditions, while further improvement was achieved by the presence of tungsten. The coatings produced in tungstate containing bath using the bipolar waveform with 40% cathodic duty cycle provided the best performance in both sliding conditions, showing ~90% reduction in volume loss comparing to the coating produced in additive-free electrolyte using unipolar waveform.

## 1. Introduction

Aluminum and its alloys are widely used due to a combination of properties, such as high strength-to-weight ratio, high thermal and electrical conductivity, and easy machinability. These features make aluminum alloys election materials for automotive industries in order to increase fuel consumption efficiency through weight reduction of the components [1]. Moreover, 7075 Al alloy has been widely used in thick-section airframe components due to superior combination of strength and fracture toughness [2], even if low wear and corrosion resistance of this alloy represents a significant drawback for its applications [3].

Among the surface treatments proposed to overcome this problem, Plasma Electrolytic Oxidation (PEO) is one of the most promising allowing for the growth of oxide ceramic coatings on light alloys such as Ti, Al, and Mg [4]. PEO is an eco-friendly process based on conventional anodic oxidation in aqueous electrolytes. This treatment is operated above the breakdown voltage and produces thicker and more adherent oxide layers than the conventional and hard anodizing [5, 6]. Moreover, PEO can also change the color of the alloy surface necessary for aerospace applications [7].

Plasma electrolytic oxidation is a versatile process that allows for tailoring the morphology, structure and composition of the coatings by tuning the electric regime (i.e. current type, current density, duty cycle) as well as the electrolytic bath composition (i.e. pH, additives presence and concentration, etc) [8, 9]. PEO treatments are commonly carried out applying direct current (DC), alternating current (AC), and pulsed current (PC) [10]. It has been proved that the coatings obtained using DC are highly porous and can be easily detached from the substrate. Applying AC, despite providing more adhesive and less porous oxide coatings, is not of industrial interest due to low growth rate and low energy efficiency during coating production [11]. Conversely, PC produces more compact and adherent layers with improved tribocorrosion and wear resistance by changing the

nature of plasma discharges [12, 13]. According to literature [14, 15], the initial pulse delay and the cathodic cycle are two important factors for PC usage superiority. The presence of cathodic duty cycle randomizes the discharges on metal surface and when increased to obtain a soft-sparking condition, the formed coatings become more uniform in thickness and roughness [16]. This uniformity is the result of the controlled discharges and the sealing effect of cathodic polarization, during which the remained cracks and channels from anodic breakdown are sealed [17]. Notably, in [18] it has been shown that the wear resistance of 6061 Al alloys can be improved by PEO coating produced using bipolar pulsed current mode with high negative peak current.

On the other hand, a crucial role is played by the electrolyte, since foreign species derived from the bath can be incorporated into the coating during PEO process with consequent changes in the structure, composition, and porosity of the layers [19]. Metal salts additives such as  $\text{KMnO}_4$  [20],  $\text{NH}_4\text{VO}_3$  [21], and  $\text{K}_2\text{TiF}_6$  [22] are usually employed as oxidizing and colouring agents, sodium tungstate ( $\text{Na}_2\text{WO}_4$ ) enhances the hardness of the coating according to [23]. Additionally, tungsten-containing coatings formed by constant current density on 8011 and 6061 Al alloys revealed enhanced corrosion resistance [24, 25].

In a previous work [26], we have studied the W incorporation mechanism during plasma electrolytic oxidation of 7075 Al alloys employing different electric regimes. The experimental findings reported in this paper proved that incorporation of W in PEO coatings grown under a soft sparking regime has a beneficial effect on the corrosion resistance of the alloy in highly aggressive environments. Starting from these experimental findings, this work is aimed to assess the influence of pulsed current waveforms alongside the incorporation of sodium tungstate as an additive on wear resistance of 7075 Al alloy. Unipolar and bipolar current modes with two different cathodic/anodic pulse ratios were used in aqueous solutions without and with tungstate addition. Tribocorrosion and dry sliding tests were executed to study and compare the wear behavior of coatings.

## 2. Experimental procedure

7075 Al alloys from a T6-heat treated rod with the chemical composition (wt%) of 5.1 Zn, 2.2 Mg, 1.2 Cu, 0.3 Fe, 0.2 Si, 0.2 Cr, 0.2 Mn, and balance Al were used as substrates in cylindrical shape with 2 cm diameter and 1 cm height. The samples were then ground using SiC papers from 600 to 2400 grit and polished until a surface roughness of  $R_a < 0.1 \mu\text{m}$  was achieved. After being degreased in acetone, the specimens were rinsed in distilled water and dried by warm air blowing. Finally, the samples were connected to copper wires and covered on the sides in order to prevent oxide growth on these areas.

Plasma electrolytic oxidation was carried out in two silicate baths ( $10 \text{ g l}^{-1}$  sodium silicate and  $2 \text{ g l}^{-1}$  potassium hydroxide) without (B1) and with  $3 \text{ g l}^{-1}$  sodium tungstate (B2) [26, 27], using three waveforms: unipolar (W1) and bipolar regimes with 20 (W2) and 40% (W3) cathodic duty cycles according to our previous studies [26, 27]. A schematic representing the coating system is illustrated in figure 1. The cell is equipped with a centrifugal pump for stirring, thermostat controller and a reciprocating compressor chiller to keep the operation temperature at  $25 \pm 1 \text{ }^\circ\text{C}$ . Two stainless steel sheets ( $30 \text{ cm} \times 30 \text{ cm}$ ) on the bath sides were used as the counter electrodes. The selection of electrical parameters were according to our previous studies [26, 27].

Surface morphology of the coatings, as well as their cross-sections, were investigated by scanning electron microscope (SEM, Philips XL30). The surface roughness of the coatings was measured using a profilometer (model Mitutoyo SJ 210), which was also used to determine the worn area depth after the tests. Tribocorrosion tests were carried out in a reciprocating ball-on-flat tribometer in presence of 3.5 wt% NaCl solution at pH 4 adjusted by hydrogen chloride. 10 N of loading was used on a SiC ball with 3 mm diameter as the counterpart material oscillating a 7 mm amplitude at 1 Hz frequency. Before running the process, each specimen was immersed in the solution for 1 h in order to achieve a stable open circuit potential (OCP). The variations in potential were recorded 15 min before sliding, during sliding (45 min) and 15 min after sliding using saturated Ag/AgCl as reference electrode, Pt plate as counter electrode and specimen as working electrode connected to an EG&G potentiostat/galvanostat (model 263A). The samples were ultrasonically cleaned and dried by warm blowing prior to observing the wear tracks using SEM and measuring the volume loss by profilometer. The same tribometer was used to conduct wear test in the air at ambient temperature (20% humidity). In this case, 2 N of loading was used on the mentioned ball reciprocating in the same manner for 45 min. Coefficient of friction (COF) was recorded using a dynamometer connected to the computer during dry wear tests.

## 3. Results and discussion

### 3.1. Coating characterization

According to our previous works [26, 27], the coatings were mainly composed of  $\gamma$ -alumina for both sets of tungsten-free and tungsten-containing coatings. Metallic tungsten was also present in the coatings treated in tungstate-containing electrolyte. The main elements of the coatings produced in additive-free bath were Al, O,

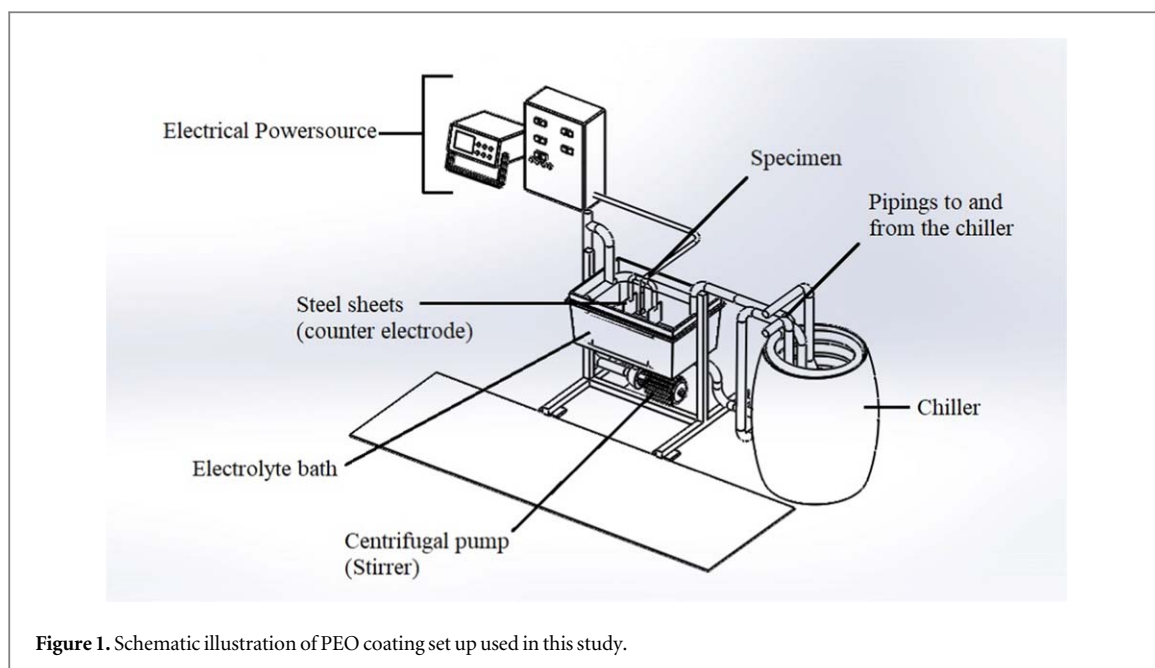


Figure 1. Schematic illustration of PEO coating set up used in this study.

Table 1. Coatings thickness and average value of surface roughness (Ra) and the value between the highest peak and the deepest valley (Rz).

Sample	Thickness ( $\mu\text{m}$ )	Ra ( $\mu\text{m}$ )	Rz ( $\mu\text{m}$ )
B1W1	24.14 $\pm$ 4.1	2.66	22.86
B1W2	28.05 $\pm$ 10.7	3.11	28.12
B1W3	35.11 $\pm$ 10.8	4.00	36.52
B2W1	20.02 $\pm$ 5.7	2.94	23.75
B2W2	26.40 $\pm$ 5.1	3.80	25.13
B3W3	24.03 $\pm$ 7.9	4.54	31.01

and Si, while W was also present in the coatings grown in tungstate-containing bath. By applying the bipolar current regimes, both W and Si contents of the coatings reduced significantly. In this case, the W contents were 2.6 and 0.8 at% for the coatings grown by unipolar and bipolar waveforms, respectively [26].

According to SEM observations (figure 2), the unipolar waveform results in the formation of pancake-like surface morphology, whereas applying the bipolar waveforms promotes the volcano-like morphology. A high level of porosity was created in the coatings produced by the unipolar waveform, and a pore-band was detected at the coating/substrate interface even in presence of tungstate (figure 2(d')). However, application of the bipolar waveforms resulted in the formation of more compact coatings restating its advantage over unipolar waveform [21, 22]. Table 1 shows the thickness and roughness of the coatings. B1W1, B1W2, and B1W3 are the coatings produced in the tungstate-free bath using unipolar (W1) and bipolar waveforms (W2 and W3) [27], where, B2W1, B2W2 and B2W3 coatings are grown accordingly in the tungsten-containing bath [26]. The data reported in table 1 reveals that using the bipolar waveforms induces an increase of the coating thickness and roughness for both sets of coatings. Moreover, the average roughness values tend to be close to each other in the coatings obtained by the same waveform from both tungstate-containing and tungstate-free baths.

### 3.2. Wear and tribocorrosion tests

The dependence of the coefficient of friction (COF) as a function of the sliding distance during dry wear process of the coatings is illustrated in figure 3. COFs are almost constant without transition points indicating that the ball does not touch the metallic substrate. COFs of the coatings grown by the bipolar waveforms are higher than those measured for coating grown by unipolar mode, due to the higher roughness originated from the volcano-like morphology. In some cases (e.g. B1W3 and B2W1 coatings), gradual increase in COF is observed. This could be ascribed to the particles spalling from the surface and debris accumulation at scar edge, which intensify the wear damage and lead to the increase of COF. Overall, slightly higher COFs are obtained for the tungsten-containing coatings.

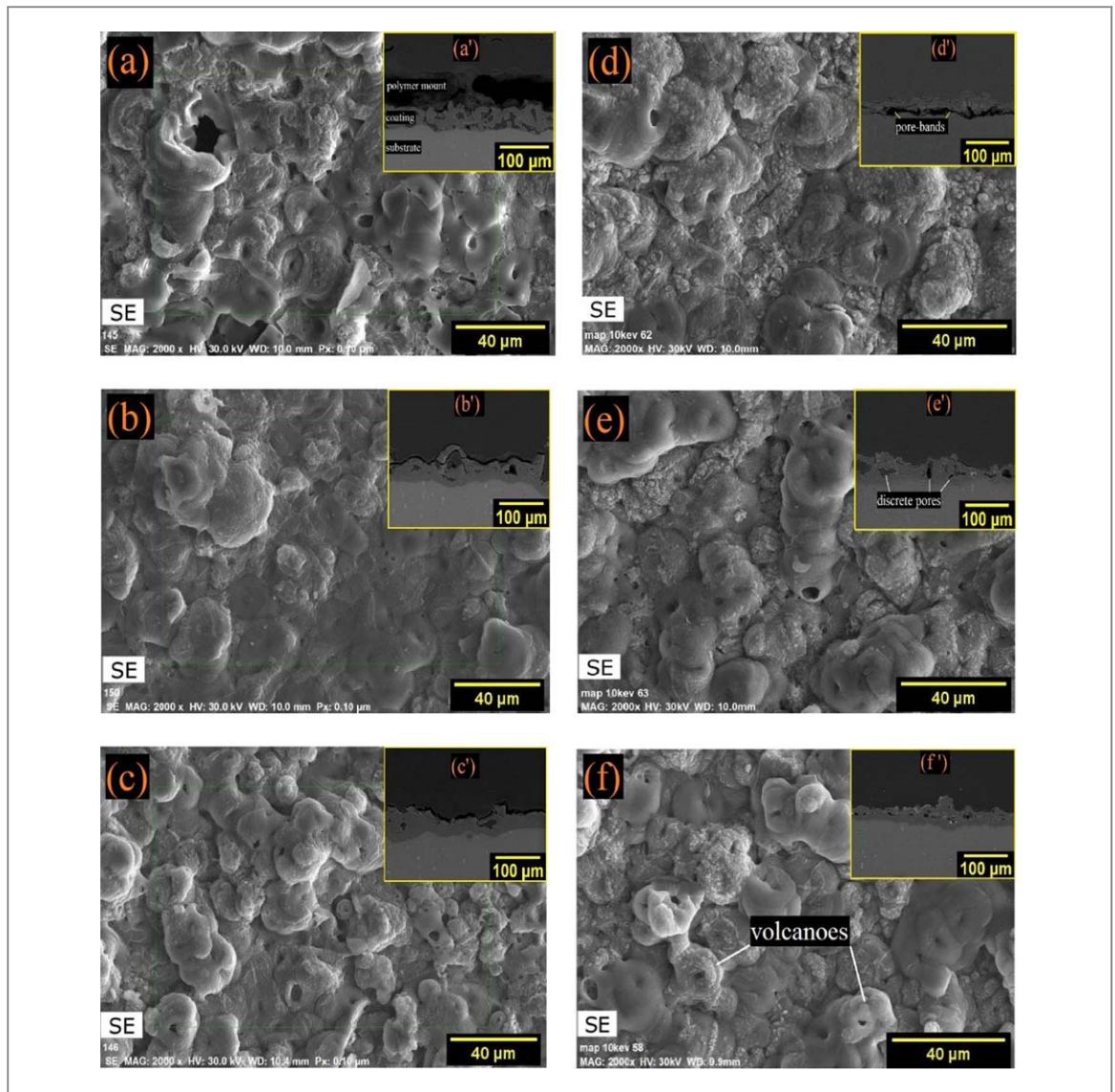


**Figure 2.** SEM images from surface and cross-section of tungsten-free and tungsten-containing coatings using unipolar and bipolar waveforms, respectively: (a, a') B1W1, (b, b') B1W2, (c, c') B1W3, (d, d') B2W1, (e, e') B2W2 and (f, f') B2W3.

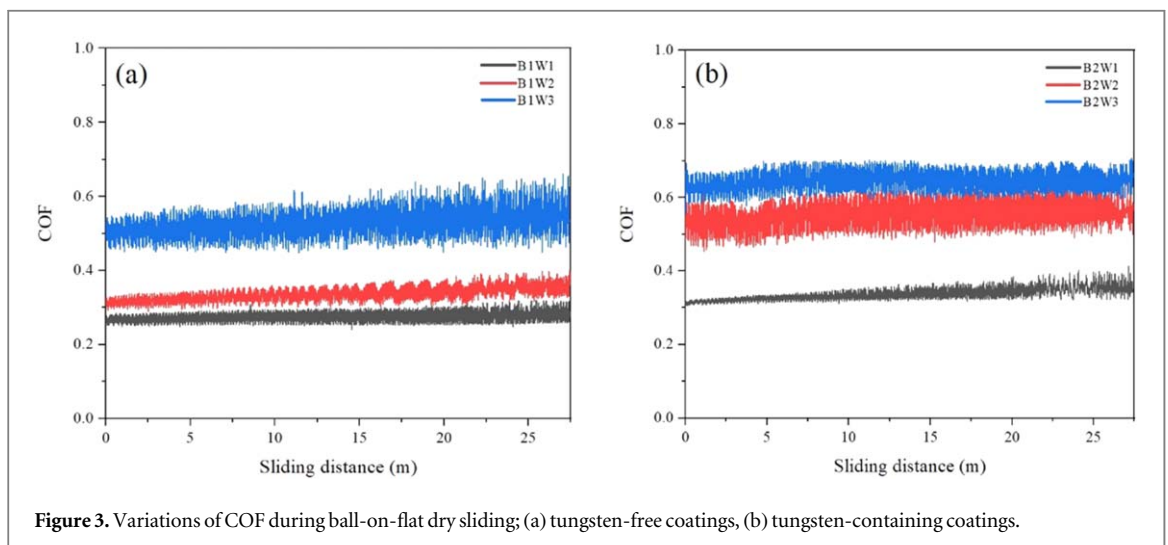


**Figure 3.** Variations of COF during ball-on-flat dry sliding; (a) tungsten-free coatings, (b) tungsten-containing coatings.

For the tribocorrosion test, the OCPs of the coatings were recorded continuously versus immersion time in 3.5% NaCl solution (figure 4). Each graph reveals three regions including pre-sliding (15 min), during-sliding (45 min) and post-sliding (15 min) as shown in the diagram. It is evident that the coatings produced by the



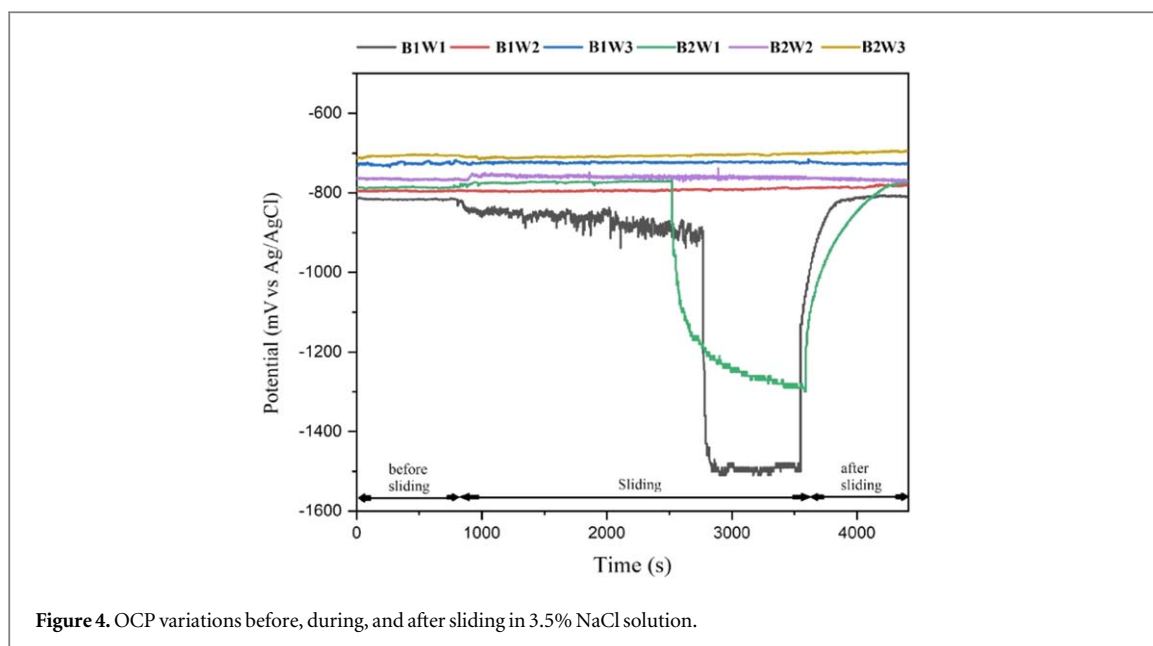


Figure 4. OCP variations before, during, and after sliding in 3.5% NaCl solution.

unipolar waveform cannot resist against 10 N loading as their OCP values drop after about 30 min of sliding. The deterioration of PEO layer exposes Al substrate to the aggressive solution, and thus, reveals a potential drop. After sliding, the potential starts rising to less negative values illustrating that the galvanic couple has been shut down by Al repassivation [28]. Earlier OCP drop of B2W1 could be related to the presence of pore-band in its oxide/substrate interface. In this case, the OCP decreased continuously after its sudden drop until the end of sliding. This indicates that the area of the active region (i.e. bare Al alloy substrate) is increasing gradually in the worn track during the sliding. However, the OCP remained constant after its sudden drop for B1W1 sample. This situation is more likely raised by the pore-band structure in B2W1 sample, but does not exist in tungsten-free (B1W1) one. It seems that the pore-band prevents SiC ball to uniformly contact the Al substrate surface for B2W1 coating. Moreover, the ball rubbing the surface of B1W1 causes strong fluctuations before the potential drop, which are raised by intensive delamination of tribo-layers [24, 25], more likely due to the presence of a high level of pores.

The coatings formed using the bipolar waveforms experienced no potential drop during sliding. The asperities on these coatings provide stable tribo-layers by mechanical interlocking that are able to protect the coating from detachment, while tribo-layers lack adherence in the coatings grown by unipolar waveform [29]. Similar results have been obtained for the PEO coatings grown in the presence of potassium titanate using the similar waveforms [12]. In the presence of titanate, the coatings produced by the bipolar waveforms also showed no potential drop during sliding, while the coating grown by the unipolar waveform revealed a potential drop indicating the coating removal inside the wear scar [12]. Comparison of the OCP variations indicates the advantage of bipolar waveforms over the unipolar one on obtaining the coatings withstand degradation during sliding in aggressive media.

The wear scars were scanned using SEM in order to determine the width and the surface morphology of the worn areas. By using the line profiles from wear scars after tribocorrosion and dry sliding, the shape of the scars, and thus, volume loss of the scars was calculated. The volume loss of worn areas was calculated by integrating the line profiles and the results along with the coating hardness values are presented in table 2. According to that, B1W1 demonstrates the highest volume loss ( $520 \times 10^{-3} \text{ mm}^3$ ) with maximum scar depth of  $55 \mu\text{m}$  in the tribocorrosion test. In spite of the presence of pore-band, B2W1 revealed lower damage during rubbing by SiC ball ( $299 \times 10^{-3} \text{ mm}^3$ ), probably due to its higher hardness resulted by the presence of tungsten in its structure. However, in both sets, we can see a restorative trend in lost material by changing to bipolar waveforms. As previously stated, using the bipolar waveforms prevents the formation of pores especially at coating/substrate interface which surely enhances hardness and adhesion of the coatings.

As seen in table 2, the bipolar waveforms have guaranteed higher hardness, and hence, better wear resistance in agreement with previous studies [12, 30]. Moreover, introducing tungsten has effectively raised the coating hardness. For these two reasons, the tungsten-containing coating grown using the bipolar waveform with the widest negative cycle (i.e. B2W3) reveals the lowest volume loss ( $8 \times 10^{-3} \text{ mm}^3$ ) in the tribocorrosion test. A similar trend is observed in dry wear analysis (table 2). However, for the coatings grown by the bipolar waveforms, the volume loss in dry sliding at 2 N loading is almost close to that in the tribocorrosion test (10 N

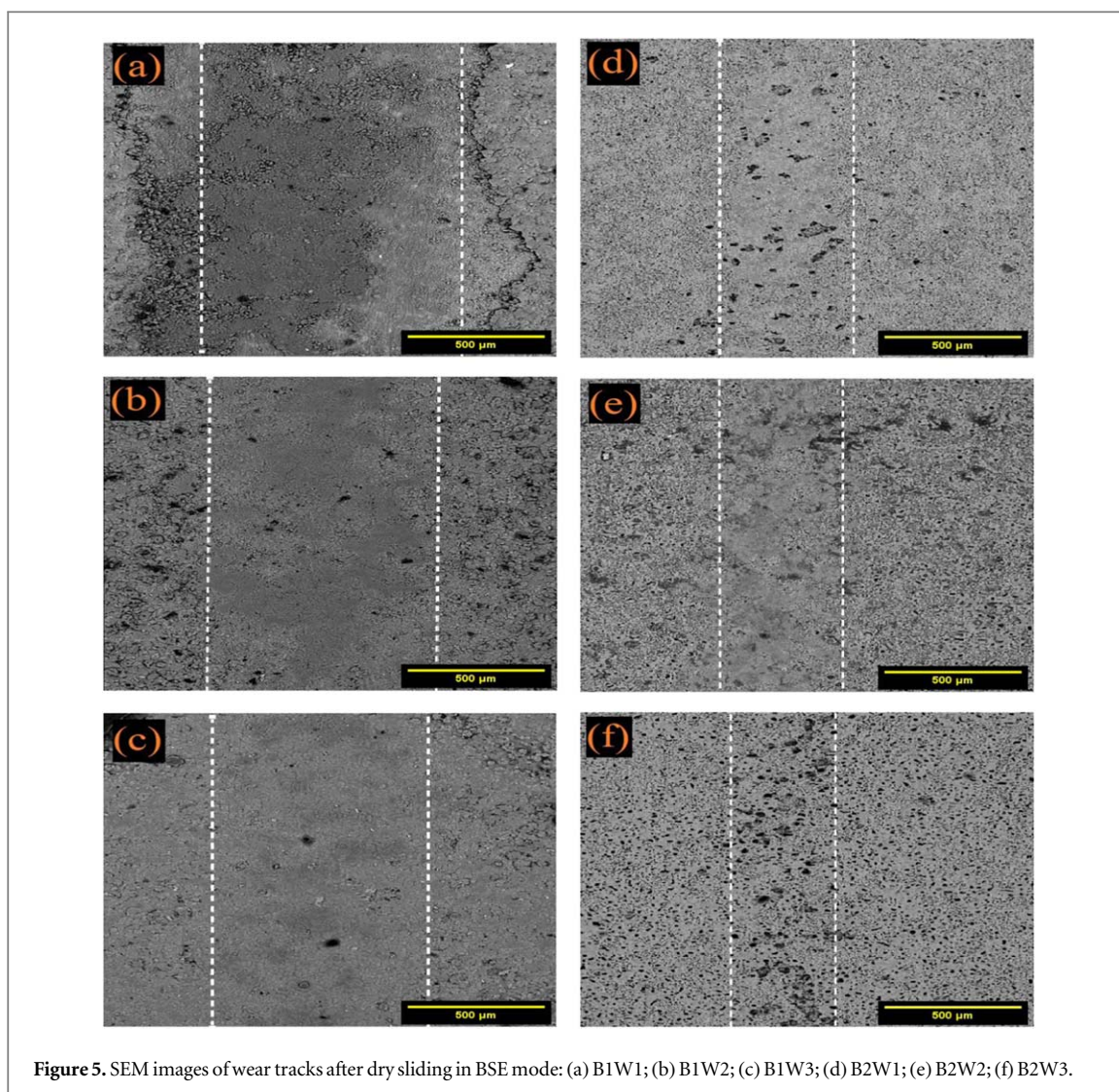


**Figure 5.** SEM images of wear tracks after dry sliding in BSE mode: (a) B1W1; (b) B1W2; (c) B1W3; (d) B2W1; (e) B2W2; (f) B2W3.

**Table 2.** Hardness of the coatings and wear track analysis results.

Sample code	Hardness (Hv)	Wet sliding		Dry sliding		Average COF
		Volume loss ( $\times 10^{-3}$ mm <sup>3</sup> )	Max. depth ( $\mu$ m)	Volume loss ( $\times 10^{-3}$ mm <sup>3</sup> )	Max. depth ( $\mu$ m)	
B1W1	912	520	55	170	33	0.27
B1W2	1521	81	19	83	20	0.33
B1W3	1924	16	13	15	10	0.52
B2W1	1152	299	42	135	26	0.34
B2W2	1795	64	17	54	15	0.55
B2W3	2297	8	7	5	4	0.64

loading). This suggests that the aggressive solution present in surface pores has delayed the wear process. It is reported in the literature [29] that the solution film redistributes the stresses over the surface and reduces the wear when removed sequentially by sliding. In this way, instead of severe wear of the coating expected at 10 N loading, it is the solution film being removed and provides a low-shear layer against rubbing as described in [29]. On the contrary, a significant difference in volume loss can be distinguished for the coatings produced by the unipolar waveform (i.e. B1W1 and B2W1) when compared in dry and wet sliding conditions. This difference indicates that the contribution of corrosion is probably high in these two coatings more likely because of their higher porosity as described before.

SEM micrographs of worn surfaces after both dry and wet sliding conditions are shown in figures 5 and 6, respectively. The wear tracks of the coatings formed by unipolar waveform can easily be detected due to intense



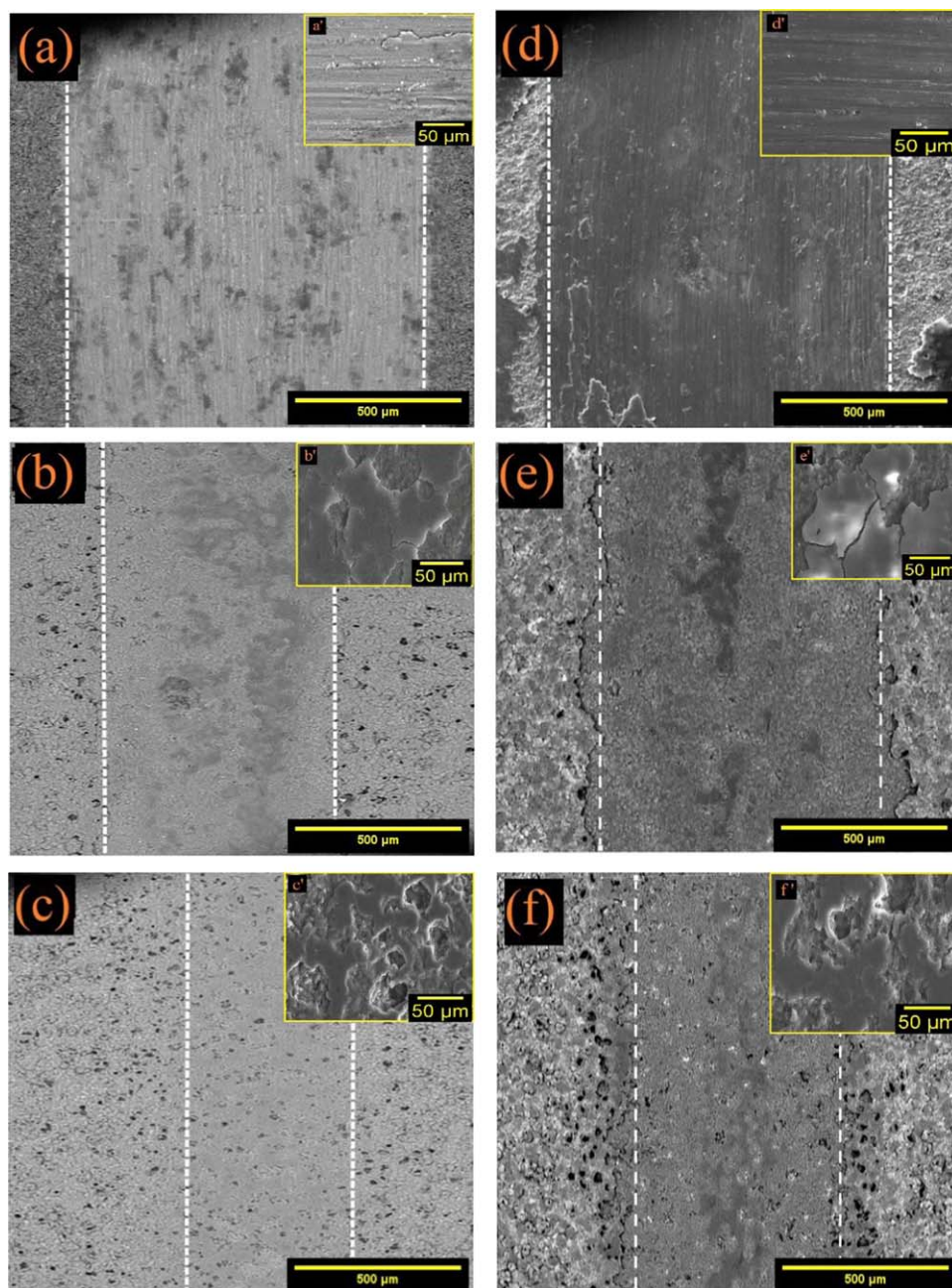


**Figure 6.** SEM images of wear tracks after tribocorrosion in BSE and higher magnification in SE modes, respectively: (a, a') B1W1; (b, b') B1W2; (c, c') B1W3; (d, d') B2W1; (e, e') B2W2; (f, f') B2W3.

damage, while they become less distinctive in coatings formed by the bipolar waveforms. The worn areas are specified by dotted lines confirming the reduction of the wear track width by altering the applied waveform and adding tungsten. Deformed areas are created outside the wear tracks very close to the edges. It seems that the coating fracture and delamination have occurred due to low load-carrying of coatings as it is subjected to shear stresses exceeded than the yield strength [31]. According to [32, 33], during PEO treatment, internal stresses could be generated by rapid solidification of ejected material from discharge channels or uneven thermal expansion of the coating and substrate. These stresses which found to be compressive in nature, effectively reduce the shear stresses on the surface and avoid microcracking during the wear process.

During the dry wear (figure 5), porous part of the coatings is detached and damages the surface in a third-body abrasion manner. Thus, the prevailing wear mechanism in dry condition seems to be three-body abrasive and micropolishing [29, 34, 35], while the formation of tribo-layer is predominant in tribocorrosion (figure 6) [30, 36]. As seen, using the wider negative cycle (W3) along with the tungstate additive in PEO treatment of 7075 Al alloy provides it a higher wear and wear-corrosion resistance.



## 4. Conclusions

7075 Al alloy specimens were coated by plasma electrolytic oxidation process using unipolar and bipolar pulsed currents in absence and presence of sodium tungstate. Waveforms varied from 0 to 20 and 40% cathodic duty cycle impacting the surface morphologies greatly beside mechanical properties.

Using the unipolar waveform, the high porosity level created in the coatings were detrimental for tribocorrosion resistance as OCP drop was observed during sliding. However, adding sodium tungstate resulted in enhanced wear resistance by decreasing the lost volume from 170 to 135 ( $\times 10^{-3} \text{ mm}^3$ ) in dry condition and from 520 to 229 ( $\times 10^{-3} \text{ mm}^3$ ) in 3.5% NaCl solution due to increased hardness of the coating from 912 to 1152 Hv. It was found that the PEO treating using the bipolar waveform with the wider cathodic width besides adding sodium tungsten to the electrolyte results in the formation of the most proper coating showing the least volume losses in tribocorrosion ( $8 \times 10^{-3} \text{ mm}^3$ ) and dry sliding ( $5 \times 10^{-3} \text{ mm}^3$ ).

## Acknowledgments

Supports from Isatic Nano plating Co. and from Università degli Studi di Palermo (bando CORI 2016 Azione D) are gratefully acknowledged. In addition, authors are thankful from Yekta Mobaddel Pars Co. for programming the waveforms.

## ORCID iDs

Amirhossein Toulabifard  <https://orcid.org/0000-0002-8238-0849>

Keyvan Raeissi  <https://orcid.org/0000-0002-1380-6551>

## References

- [1] Heymes F, Commet B, Du Bost B, Lassince P, Lequeu P and Raynaud G M 1997 *Development of new Al alloys for distortion free machined aluminium aircraft components* (USA: ASM International) pp 249–55
- [2] Finney J M 1994 *Fatigue Crack Growth in Metallic Military Aircraft Structures Handbook of Fatigue Crack: Propagation in Metallic Structures* ed A Carpinteri 2 (The Netherlands: Elsevier Science B.V.) 1539–65
- [3] von Hehl A and Krug P 2013 *Aluminum and Aluminum Alloys Structural Materials and Processed in Transportation* (Singapore: Wiley-VCH) ch 2, pp 49–112
- [4] Mohedano M, Lu X, Matykina E, Blawert C, Arrabal R and Zheludkevich M L 2018 Plasma electrolytic oxidation (PEO) of metals and alloys ed K Wandelt *Interfacial Chem.* (Oxford: Elsevier) pp 423–38
- [5] Treviño M, Garza-Montes-de-Oca N F, Pérez A, Hernández-Rodríguez M A L, Juárez A and Colás R 2012 Wear of an aluminium alloy coated by plasma electrolytic oxidation *Surf. Coatings Technol.* **206** 2213–9
- [6] Khorasanian M, Dehghan A, Shariat M H, Bahrololoom M E and Javadpour S 2011 Microstructure and wear resistance of oxide coatings on Ti-6Al-4V produced by plasma electrolytic oxidation in an inexpensive electrolyte *Surf. Coatings Technol.* **206** 1495–502
- [7] Yeh S C, Tsai D S, Wang J M and Chou C C 2016 Coloration of the aluminum alloy surface with dye emulsions while growing a plasma electrolytic oxide layer *Surf. Coatings Technol.* **287** 61–6
- [8] Walsh F C, Low C T J, Wood R J K, Stevens K T, Archer J, Poeton A R and Ryder A 2009 Plasma electrolytic oxidation (PEO) for production of anodised coatings on lightweight metal (Al, Mg, Ti) alloys *Trans. IMF.* **87** 122–35
- [9] Jiang B L and Wang Y M 2010 Plasma electrolytic oxidation treatment of aluminium and titanium alloys *Surface Engineering of Light Alloy* ed H Dong (UK: Woodhead Publishing Limited) ch 5, pp 110–54
- [10] Li Q B, Liu C C, Yang W B and Liang J 2017 Growth mechanism and adhesion of PEO coatings on 2024Al alloy *Surf. Eng.* **33** 760–6
- [11] Yerokhin A L, Shatrov A, Samsonov V, Shashkov P, Pilkington A, Leyland A and Matthews A 2005 Oxide ceramic coatings on aluminium alloys produced by a pulsed bipolar plasma electrolytic oxidation process *Surf. Coatings Technol.* **199** 150–7
- [12] Akbari E, Di Franco F, Ceraolo P, Raeissi K, Santamaria M and Hakimzad A 2018 Electrochemically-induced TiO<sub>2</sub> incorporation for enhancing corrosion and tribocorrosion resistance of PEO coating on 7075 Al alloy *Corros. Sci.* **143** 314–28
- [13] Li Q, Liang J, Liu B, Peng Z and Wang Q 2014 Effects of cathodic voltages on structure and wear resistance of plasma electrolytic oxidation coatings formed on aluminium alloy *Appl. Surf. Sci.* **297** 176–81
- [14] Jin F, Chu P K, Xu G, Zhao J, Tang D and Tong H 2006 Structure and mechanical properties of magnesium alloy treated by micro-arc discharge oxidation using direct current and high-frequency bipolar pulsing modes *Mater. Sci. Eng. A* **435–436** 123–6
- [15] Jaspard-Mécuson F, Czerwiec T, Henrion G, Belmonte T, Dujardin L, Viola A and Beauvir J 2007 Tailored aluminium oxide layers by bipolar current adjustment in the plasma electrolytic oxidation (PEO) process *Surf. Coatings Technol.* **201** 8677–82
- [16] Rogov A B and Shayapov V R 2017 The role of cathodic current in PEO of aluminum: Influence of cationic electrolyte composition on the transient current-voltage curves and the discharges optical emission spectra *Appl. Surf. Sci.* **394** 323–32
- [17] Mann R, Hansal W E G and Hansal S 2014 Effects of pulsed current on plasma electrolytic oxidation *Trans. IMF.* **92** 297–304
- [18] Gu X, Jiang B, Li H, Liu C and Shao L 2018 Properties of micro-arc oxidation coatings on aluminum alloy at different negative peak current densities *Mater. Res. Express* **5** 56522
- [19] Hussein R O, Zhang P, Nie X, Xia Y and Northwood D O 2011 The effect of current mode and discharge type on the corrosion resistance of plasma electrolytic oxidation (PEO) coated magnesium alloy AJ62 *Surf. Coatings Technol.* **206** 1990–7
- [20] Aliramezani R, Raeissi K, Santamaria M and Hakimzad A 2017 Characterization and properties of PEO coatings on 7075 Al alloy grown in alkaline silicate electrolyte containing KMnO<sub>4</sub> additive *Surf. Coatings Technol.* **329** 250–61
- [21] Li J, Cai H and Jiang B 2007 Growth mechanism of black ceramic layers formed by microarc oxidation *Surf. Coatings Technol.* **201** 8702–08

- [22] Tang M, Li W, Liu H and Zhu L 2012 Influence of  $K_2TiF_6$  in electrolyte on characteristics of the microarc oxidation coating on aluminum alloy *Curr. Appl Phys.* **12** 1259–65
- [23] Tseng C C, Lee J L, Kuo T H, Kuo S N and Tseng K H 2012 The influence of sodium tungstate concentration and anodizing conditions on microarc oxidation (MAO) coatings for aluminum alloy *Surf. Coatings Technol.* **206** 3437–43
- [24] Chen L, Han J and Yu S 2006 Preparation technology and anti-corrosion performances of black ceramic coatings formed by micro-arc oxidation on aluminum alloys *Rare Met.* **25** 146–9
- [25] Liu Y, Xu J, Gao Y, Yuan Y and Gao C 2012 Influences of additive on the formation and corrosion resistance of micro-arc oxidation ceramic coatings on aluminum alloy *Phys. Procedia.* **32** 107–12
- [26] Hakimizad A, Raeissi K, Santamaria M and Asghari M 2018 Effects of pulse current mode on plasma electrolytic oxidation of 7075 Al in  $Na_2WO_4$  containing solution: from unipolar to soft-sparking regime *Electrochim. Acta* **284** 618–29
- [27] Hakimizad A, Raeissi K, Golozar M A, Lu X, Blawert C and Zheludkevich M L 2017 The effect of pulse waveforms on surface morphology, composition and corrosion behavior of  $Al_2O_3$  and  $Al_2O_3/TiO_2$  nano-composite PEO coatings on 7075 aluminum alloy *Surf. Coatings Technol.* **324** 208–21
- [28] Kumar S, Sankara Narayanan T S N, Ganesh Sundara Raman S and Seshadri S K 2010 Surface modification of CP-Ti to improve the fretting-corrosion resistance: thermal oxidation vs. anodizing *Mater. Sci. Eng. C* **30** 921–27
- [29] Malayoglu U, Tekin K C, Malayoglu U and Shrestha S 2011 An investigation into the mechanical and tribological properties of plasma electrolytic oxidation and hard-anodized coatings on 6082 aluminum alloy *Mater. Sci. Eng. A* **528** 7451–60
- [30] Ghafaripoor M, Raeissi K, Santamaria M and Hakimizad A 2018 The corrosion and tribocorrosion resistance of PEO composite coatings containing  $\alpha-Al_2O_3$  particles on 7075 Al alloy *Surf. Coatings Technol.* **349** 470–9
- [31] Ceschini L, Lanzoni E, Martini C, Prandstraller D and Sambogna G 2008 Comparison of dry sliding friction and wear of Ti6Al4V alloy treated by plasma electrolytic oxidation and PVD coating *Wear* **264** 86–95
- [32] Khan R H U, Yerokhin A L, Pilkington T, Leyland A and Matthews A 2005 Residual stresses in plasma electrolytic oxidation coatings on Al alloy produced by pulsed unipolar current *Surf. Coatings Technol.* **200** 1580–86
- [33] Khan R H U, Yerokhin A, Li X, Dong H and Matthews A 2010 Surface characterisation of DC plasma electrolytic oxidation treated 6082 aluminium alloy: effect of current density and electrolyte concentration *Surf. Coatings Technol.* **205** 1676–88
- [34] Mu M, Liang J, Zhou X and Xiao Q 2013 One-step preparation of  $TiO_2/MoS_2$  composite coating on Ti6Al4V alloy by plasma electrolytic oxidation and its tribological properties *Surf. Coatings Technol.* **214** 124–30
- [35] Cao G P and Song R G 2018 Microstructure and properties of ceramic coatings prepared by micro-arc oxidation on 7075 aluminum alloy *Mater. Res. Express* **5** 26407
- [36] Arrabal R, Mohedano M, Matykina E, Pardo A, Mingo B and Merino M C 2015 Characterization and wear behaviour of PEO coatings on 6082-T6 aluminium alloy with incorporated  $\alpha-Al_2O_3$  particles *Surf. Coatings Technol.* **269** 64–73